



Cite this: *Chem. Commun.*, 2019, 55, 1259

Received 21st November 2018,
Accepted 2nd January 2019

DOI: 10.1039/c8cc09253b

rsc.li/chemcomm

Directing GDNF-mediated neuronal signaling with proactively programmable cell-surface saccharide-free glycosaminoglycan mimetics†

Shuting Cai,^{‡a} Daniel H. Lukamto,^{‡a} Jerry K. C. Toh,^{§a} Roland G. Huber,^{id b} Peter J. Bond,^{id bc} Joo-Eun Jee,^a Teck Chuan Lim,^{id a} Pei Liu,^a Liwei Chen,^a Qianqian Vicky Qu,^a Su Seong Lee^{id a} and Song-Gil Lee^{id *a}

A significant barrier to harnessing the power of cell-surface glycosaminoglycans (GAGs) to modulate glial cell-line-derived neurotrophic factor (GDNF) signaling is the difficulty in accessing key GAG structures involved. Here, we report tailored GDNF signaling using synthetic polyproline-based GAG mimetics (PGMs). PGMs deliver the much needed proactive programmability for GDNF recognition and effectively modulate GDNF-mediated neuronal processes in a cellular context.

The ability to systematically modulate growth factor signaling presents a powerful means to lead the fate of a cell to a specific desired state, raising the prospect of realizing revolutionary and highly controllable cell-based therapies.

GDNF has drawn prominent attention for its inherent regulatory capacity to activate clinically relevant signaling cascades, the dysfunction of which is directly implicated in disease states.^{1–3} Ever since the groundbreaking discovery of GDNF⁴ and its function in dopaminergic neurons,^{4,5} its critical contribution to the differentiation and maintenance of various neurons has been widely recognized. GDNF has thus emerged as a highly promising therapeutic option in the battle against several devastating neurological diseases including Parkinson's disease.² However, despite intense efforts over the past two decades, translation of its therapeutic potential into the clinical setting has yet to be fully realized, in large part due to poor clinical efficacy and off-target side effects.^{6–8} Hence, there have

been increasing demands for adjuvant strategies to overcome the shortcomings of current GDNF-based therapeutic approaches.

From the mechanistic perspective, cellular responses to GDNF are primarily defined by the multicomponent receptor complexation with its membrane-associated GDNF family receptor $\alpha 1$ (GFR $\alpha 1$) and Ret receptor tyrosine kinase (RET).^{2,9} Importantly, several inspiring investigations have revealed that GAGs such as heparan sulfate (HS) present on cell-surface proteoglycans constitute the central axis for facilitating this complexation by engaging GDNF in the vicinity of its cell-surface receptors in a carefully regulated fashion.^{10,11} Conversely, enzymatic deletion of cell-surface GAG leads to the shutdown of GDNF signaling,¹⁰ providing firm evidence that GAG is indeed an indispensable element for retaining GDNF bioactivity. Taken together, we reasoned that harnessing cell-surface GAG–GDNF interactions could open up opportunities to devise a powerful adjuvant strategy for potentiating GDNF signaling, while negating undesirable signaling outputs, by adding another layer of biospecific linkage between GDNF and its cell-surface receptors. Herein, we report the first case of controlled glycocalyx editing to display proactively programmable GAG mimicking sulfated constructs in the context of GDNF on the cell-surface. The present communication details its impact on modulating GDNF activity and defining the outcome of GDNF-mediated neuronal signaling events in cellular environments.

Our design concept for GDNF-binding GAG mimetics began with the critical selection of an appropriate mimetic toolbox. While specific types of sulfation patterns have long been considered central to underpin GAG function to engage GDNF,^{12–14} the fundamental difficulty of thoroughly mapping GDNF-recognizing sequences lies in the chemical complexity and diversity of GAG *in vivo*. As such, the full structural details of GAG involved are not yet available. As a compelling solution to such problems, we recently reported a new paradigm for engineering saccharide-free PGMs which subscribe to a helical, periodic format much like GAGs, but which: (i) are easily accessible, (ii) are devoid of complex structural fluctuations and therefore (iii) hold sulfate moieties in discrete, independent positions in 3D space.¹⁵

^a Institute of Bioengineering and Nanotechnology, 31 Biopolis Way, The Nanos, Singapore 138669, Singapore. E-mail: sglee@ibn.a-star.edu.sg

^b Bioinformatic Institute, 30 Biopolis Street, #07-01 Matrix, Singapore 138671, Singapore

^c Department of Biological Sciences, National University of Singapore, 14 Science Drive 4, Singapore 117543, Singapore

† Electronic supplementary information (ESI) available: Experimental details, compound characterization, and supporting tables, figures and schemes. See DOI: 10.1039/c8cc09253b

‡ These authors contributed equally to this work.

§ Current address: NanoBio Lab, 31 Biopolis Way, The Nanos, #09-01, Singapore 138669, Singapore.

We envisioned that this platform would be particularly useful to develop GAG mimetics for targeting GDNF owing to its unique ability to proactively program desired macromolecular sulfate displays and manipulate protein interactions systematically even with little information about the sulfation patterns of natural GAGs involved. Previous studies have revealed that sulfate groups on natural GAGs can either partition circumferentially onto multiple sides or line up on one single side of their helical backbone.^{16–18} To sample some of these configurations and identify a suitable sulfate display for GDNF recognition, we herein generated four distinct biotinylated PGMs carrying 24 sulfate moieties, namely **B- $\{Z\}_{12}$** , **B- $\{PZZ\}_6$** , **B- $\{PPZ\}_{12}$** and **B- $\{PPZZ\}_6$** , which partition sulfate groups onto 3 sides, 2 sides, 1 side or 3 sides (with alternate pairs of 2 sulfated prolines and 2 prolines), respectively (Fig. 1A). Circular dichroism (CD) measurements demonstrated that all PGMs adopted the typical polyproline type II helical profiles with a maximum positive band at 225–228 nm and a minimum negative band at 208 nm confirming that the secondary structure of the polyproline scaffold was little influenced by the presence of sulfate moieties (Fig. 1B).¹⁹

Having successfully prepared PGMs and characterized their 3D structures, our next task was to examine whether PGMs would be effective in recruiting GDNF using surface plasmon resonance (SPR). Biotinylated PGMs or natural HS (~26 sulfate moieties) was immobilized on streptavidin-coated sensor chips and the interactions were examined as a function of GDNF concentration. The sensorgrams in Fig. 2 showed that despite all PGMs carrying an equal number of sulfate groups, switching across PGMs in the order of **B- $\{PPZZ\}_6$** , **B- $\{PPZ\}_{12}$** , **B- $\{PZZ\}_6$** and

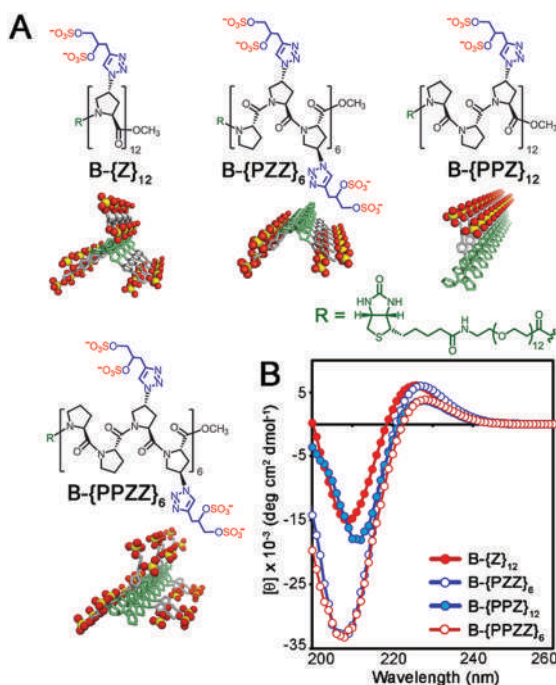


Fig. 1 (A) Chemical structures and 3D depictions of PGMs. (B) CD spectra of PGMs.

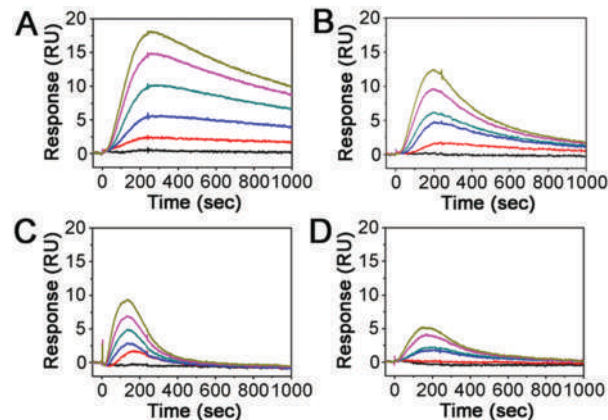


Fig. 2 SPR sensorgrams for GDNF binding at various GDNF concentrations. (From top to bottom: 1.2, 1.0, 0.8, 0.6, 0.4 and 0.2 nM). (A) **B- $\{Z\}_{12}$** , (B) **B- $\{PZZ\}_6$** , (C) **B- $\{PPZ\}_{12}$** and (D) **B- $\{PPZZ\}_6$** . Complete kinetic parameters are shown in Table S1 (ESI[†]).

B- $\{Z\}_{12}$ progressively increased the binding affinity toward GDNF. Specifically, GDNF was effectively recognized by both **B- $\{Z\}_{12}$** and **B- $\{PZZ\}_6$** , characterized by a slow initial association rate that rapidly reached equilibrium followed by a slow dissociation rate (Fig. 2A and B). However, a comparison of K_D values illustrated that the ability of **B- $\{Z\}_{12}$** to recruit GDNF ($K_D = 3.30$ nM) was greater than that of **B- $\{PZZ\}_6$** ($K_D = 12.4$ nM) by approximately 4-fold, mainly attributed to its relatively fast association rate compared to **B- $\{PZZ\}_6$** (Table S1, ESI[†]). It is noteworthy that both **B- $\{Z\}_{12}$** and **B- $\{PZZ\}_6$** outperformed natural HS ($K_D = 81.93$ nM) for GDNF binding (Fig. S9 and Table S1, ESI[†]), suggesting that PGMs can serve as a compelling alternative to heterogeneous GAGs derived from natural sources for attaining an effective ligand for GDNF. We also emphasize that **B- $\{Z\}_{12}$** recruits GDNF more efficiently than a previously reported ROMP-based CS-E glycopolymer bearing a far greater number of sulfate groups (the number of sulfate groups = 194),²⁰ highlighting its superior competency to engage GDNF. K_D values could not be accurately calculated for **B- $\{PPZ\}_{12}$** and **B- $\{PPZZ\}_6$** owing to a decrease in response after reaching equilibrium in the association phase but qualitatively, they could be seen to produce substantially poorer binding affinity with slow association and fast dissociation rates (Fig. 2C and D). Collectively, two aspects of these results are particularly worth highlighting: (i) programmable sulfate displays of PGMs enabled the systematic modulation of their interactions with GDNF in a progressive fashion and thus (ii) afforded an efficient lead optimization path without *a priori* information on the necessary sulfation patterns to yield a highly effective binding ligand to GDNF $\{Z\}_{12}$.

Given the above, we further conducted unbiased molecular dynamics (MD) simulations¹⁵ to pursue a molecular-level understanding of how the $\{Z\}_{12}$ motif would interact with GDNF. We found that arbitrarily positioned $\{Z\}_{12}$ (Fig. S10A, ESI[†]) drifted toward and bound to a wide, shallow concave region of the GDNF dimer (Fig. 3A and Fig. S10B, ESI[†]). More specifically, on the basis of per-residue analysis of average molecular mechanics-generalized born surface area (MM-GBSA)²¹ interaction energies

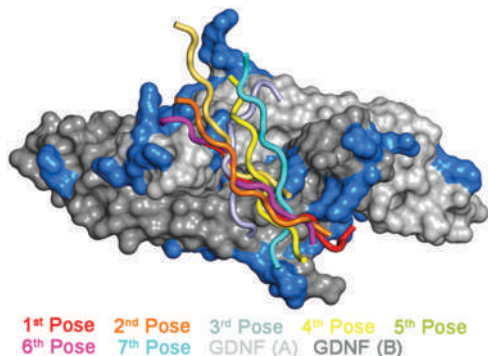


Fig. 3 Predicted top seven binding poses for $\{Z\}_{12}$ bound to the GDNF dimer as ranked by MM-GBSA analyses. $\{Z\}_{12}$ is shown as a cartoon representation for visual clarity and see Fig. S9B (ESI[†]) for full structural details. Blue color denotes basic amino acid residues.

derived from the seven most energetically favorable $\{Z\}_{12}$ /GDNF complexes, $\{Z\}_{12}$ prefers two distinct clusters of basic residues located near the interface of the GDNF dimer, namely $\{R_{112}, K_{114}, R_{116}, K_{158}, K_{161}, R_{165}, R_{167}$ and K_{173} on monomer A $\}$ and $\{R'_{112}, K'_{114}, R'_{116}, K'_{161}, R'_{165}, R'_{167}$, and K'_{173} on monomer B $\}$. The binding modes are predicted to be further strengthened by hydrogen bonding interactions with non-basic residues, namely $\{Q_{111}, N_{115}$ and S_{148} on monomer A $\}$ and $\{Q'_{176}$ on monomer B $\}$ (Fig. S10C, ESI[†]). Taken together, this modeling study demonstrates that $\{Z\}_{12}$ comprises the primary binding sites on the GDNF surface in a GAG-like manner by favoring distinct sets of electrostatic and hydrogen bonding interactions.

We next questioned whether the ability of $\{Z\}_{12}$ to recruit GDNF established in the SPR studies could be exploited to

mediate GDNF signaling in cells. To investigate this, we generated dipalmitoyl phosphatidylethanolamine (DPPE)-anchored PGMs that allow for cell-surface presentation of PGMs through passive insertion of phospholipid into the plasma membrane as reported previously (Fig. 4A).^{22,23} Rat pheochromocytoma (PC12) cells were incubated for 2 h with DPPE-anchored PGMs that had been labeled with biotin for visualization. Confocal microscopic analysis demonstrated that the DPPE-anchored PGMs were successfully inserted into the cell-surface (Fig. 4B). Moreover, **DPPE- $\{Z\}_{12}$ -B** displayed a similar level of glycocalyx remodeling to that of **DPPE- $\{Z_U\}_{12}$ -B**, enabling the quantitative comparison of their cellular activities. Consistent with previous studies by others,²³ we observed a rapid decrease in cell-surface PGMs. However, over 37% of PGMs still persisted on the cell-surface after 8 h duration, which is considered to be sufficient for the induction of RET phosphorylation to sustain intracellular signal transduction (Fig. 4B).²⁴

PC12 cells remodeled with DPPE-anchored PGMs were cultured on laminin-coated glass coverslips and neuritogenesis was triggered by adding GDNF and soluble GFR α_1 to the culture media. The neuritogenic process would be primarily mediated through the interactions of $\{Z\}_{12}$ with GDNF rather than GFR α_1 as the binding affinity of $\{Z\}_{12}$ to GFR α_1 is considerably weaker than to GDNF (Fig. S22 and Table S1, ESI[†]). The impact of **DPPE- $\{Z\}_{12}$** on neuritogenic activity of PC12 cells was significant. Neurite extension was greatly promoted and the percentage of cells bearing neurites longer than one cell body diameter was increased from 7.7% in the laminin control to 24.8%. Conversely, soluble **Ac- $\{Z\}_{12}$** added in the culture media resulted in neurite inhibition in a dose-dependent manner. This indicated that soluble **Ac- $\{Z\}_{12}$** might sequester GDNF away

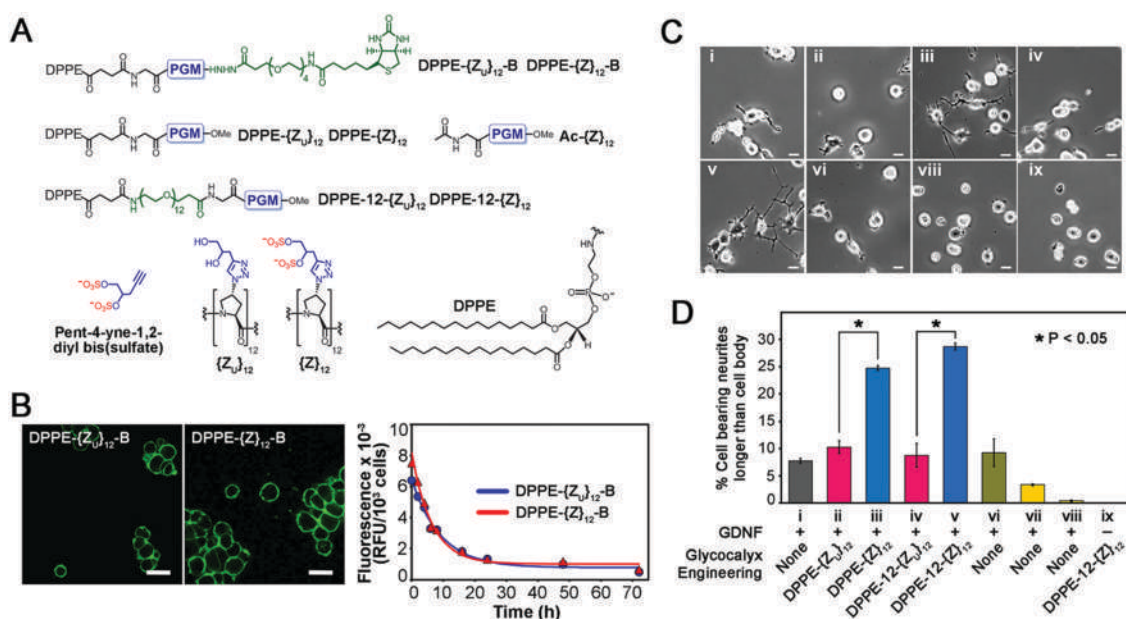


Fig. 4 (A) Chemical structures of lipid-anchored PGMs. (B) Imaging PGMs on cell membranes with Anti-Biotin Alexa Fluor-488 and cell-surface retention of **DPPE- $\{Z_U\}_{12}$** and **DPPE- $\{Z\}_{12}$** over 72 h. Scale bars = 19 μ m. (C) Representative images of PC12 neuritogenesis. Conditions used are indicated in the x-axis section of (D). Scale bars = 10 μ m. (D) Quantification of neuritogenesis. Error bars represent SD from three separate experiments. Additional reagents in culture media [vi: 1 mM of pent-4-yne-1,2-diyl bis(sulfate), vii: 10 μ M of **Ac- $\{Z\}_{12}$** , viii: 20 μ M of **Ac- $\{Z\}_{12}$**].

from the cell-surface and that $\{Z\}_{12}$ had to be inserted into the cell-surface to potentiate GDNF-mediated neurogenesis. In an attempt to optimize our glycocalyx remodeling, a PEG12 spacer was further introduced between the $\{Z\}_{12}$ motif and DPPE chain (DPPE-12- $\{Z\}_{12}$). This modification increased neurogenesis in response to GDNF to a value of 28.7%. Meanwhile, unsulfated PGMs, DPPE- $\{Z\}_{12}$ and DPPE-12- $\{Z\}_{12}$, did not exhibit any noticeable increase in neurogenic activity relative to the control, supporting the notion that a sulfate group is a prerequisite for GAG bioactivity.¹⁰ Additionally, pent-4-yne-1,2-diyl bis(sulfate) in the culture media had no discernable effect, highlighting the importance of polyvalent interactions in GDNF recognition. It is noteworthy that no neurite was detected in DPPE- $\{Z\}_{12}$ bearing cells cultured in GDNF-free medium, ruling out the possibility of a GDNF-independent neuronal process (Fig. 4C and D). Overall, these cellular observations corroborate the above protein binding and molecular modeling studies and indicate that our platform of PGMs has successfully yielded $\{Z\}_{12}$ as an effective mimetic that assumes the functions of native cell-surface GAG and sustains GDNF-mediated neuronal signal transduction.

In conclusion, the success of GDNF-based therapeutic approaches has been limited by unsatisfactory clinical effectiveness and harmful side effects.^{6–8} Our results demonstrate that saccharide-free PGMs allow for direct control and efficient optimization of the macromolecular arrangements of sulfate moieties in the context of GDNF. Even without knowing the endogenous GAG sequences involved *in vivo*, we could generate a potent GDNF binding ligand $\{Z\}_{12}$. We have further shown that the modification of the cell-surface with $\{Z\}_{12}$ can provide a robust impetus that potentiates GDNF-mediated signaling processes and amplifies the cellular responses to GDNF. This offers promise for a compelling solution to shortcomings of current GDNF-based therapeutic trials. More work lies ahead for this paradigm. For instance, as a ligand for GDNF, $\{Z\}_{12}$ may bind minimally to L-selectin and NGF but may not exhibit strong selectivity over P-selectin (Fig. S21 and Table S1, ESI†). For eventual clinical translation, selectivity has to be strengthened by either exploiting a higher diversity of sulfation displays or adding new interacting elements such as polar and hydrophobic groups. Ultimately, we anticipate that this study will provide practical and rational means toward harnessing GAG functions to engineer diverse growth factor signaling pathways with precision control and to facilitate the development of sophisticated growth factor-based therapeutics and biomaterials.

We gratefully acknowledge financial support by the Institute of Bioengineering and Nanotechnology (Biomedical Research Council, Agency for Science, Technology and Research, Singapore). We also

thank the National Supercomputing Center Singapore (www.nsc.sg) for providing computing resources.

Conflicts of interest

There are no conflicts to declare.

Notes and references

- 1 S. J. Allen, J. J. Watson, D. K. Shoemark, N. U. Barua and N. K. Patel, *Pharmacol. Ther.*, 2013, **138**, 155.
- 2 M. S. Airaksinen and M. Saarna, *Nat. Rev. Neurosci.*, 2002, **3**, 383.
- 3 D. Cortés, O. A. Carballo-Molina, M. J. Castellanos-Montiel and I. Velasco, *Front. Mol. Neurosci.*, 2017, **10**, 258.
- 4 L. F. Lin, D. H. Doherty, J. D. Lile, S. Bektesh and F. Collins, *Science*, 1993, **21**, 1130.
- 5 A. Tomac, E. Lindqvist, L. F. Lin, S. O. Ogren, D. Young, B. J. Hoffer and L. Olson, *Nature*, 1995, **373**, 335.
- 6 G. Paul and A. M. Sullivan, *Eur. J. Neurosci.*, 2018, **1**.
- 7 N. Torres, J. Molet, C. Moro, J. Mitrofanis and A. L. Benabid, *Int. J. Mol. Sci.*, 2017, **18**, 2190.
- 8 J. G. Nutt, K. J. Burchiel, C. L. Comella, J. Jankovic, A. E. Lang, E. R. Laws, A. M. Lozano, R. D. Penn, R. K. Simpson, M. Stacy, G. F. Wooten and the ICV GDNF Study Group, *Neurology*, 2003, **60**, 69.
- 9 K. M. Goodman, S. Kjaer, F. Beuron, P. P. Knowles, A. Nawrotek, E. R. Burns, A. G. Purkiss, R. George, M. Santoro, E. P. Morris and N. Q. McDonald, *Cell Rep.*, 2014, **8**, 1894.
- 10 M. W. Barnett, C. E. Fisher, G. Perona-Wright and J. A. Davies, *J. Cell Sci.*, 2002, **115**, 4495.
- 11 M. M. Bespalov, Y. A. Sidorova, S. Tumova, A. Ahonen-Bishopp, A. C. Magalhães, E. Kuleskiy, M. Paveliev, C. Rivera, H. Rauvala and M. Saarna, *J. Cell Biol.*, 2011, **192**, 153.
- 12 J. A. Davies, E. A. Yates and J. E. Turnbull, *Growth Factors*, 2003, **21**, 109.
- 13 S. M. Rickard, R. S. Mummery, B. Mulloy and C. C. Rider, *Glycobiology*, 2003, **13**, 419.
- 14 S. L. Bullock, J. M. Fletcher, R. S. P. Beddington and V. A. Wilson, *Genes Dev.*, 1998, **12**, 1894.
- 15 T. C. Lim, S. Cai, R. G. Huber, P. J. Bond, P. X. S. Chia, S. L. Khoo, S. Gao, S. S. Lee and S.-G. Lee, *Chem. Sci.*, 2018, **9**, 7940.
- 16 C. I. Gama, S. E. Tully, N. Sotogaku, P. M. Clark, M. Rawat, N. Vaidehi, W. A. Goddard, A. Nishi and L. C. Hsieh-Wilson, *Nat. Chem. Biol.*, 2006, **2**, 467.
- 17 B. Mulloy and M. J. Forster, *Glycobiology*, 2000, **10**, 1147.
- 18 J. Angulo, R. Ojeda, J. L. De Paz, R. Lucas, P. M. Nieto, R. M. Lozano, M. Redondo-Horcajo, G. Giménez-Gallego and M. Martín-Lomas, *ChemBioChem*, 2004, **5**, 55.
- 19 N. Helbecque and M. H. Loucheux-Lefebvre, *Int. J. Pept. Protein Res.*, 1982, **19**, 94.
- 20 S.-G. Lee, J. M. Brown, C. J. Rogers, J. B. Matson, C. Krishnamurthy, M. Rawat and L. C. Hsieh-Wilson, *Chem. Sci.*, 2010, **1**, 322.
- 21 S. Genheden and U. Ryde, *Expert Opin. Drug Discovery*, 2015, **10**, 449.
- 22 M. L. Huang, R. A. A. Smith, G. W. Trieger and K. Godula, *J. Am. Chem. Soc.*, 2014, **136**, 10565.
- 23 E. C. Woods, N. A. Yee, J. Shen and C. R. Bertozzi, *Angew. Chem., Int. Ed.*, 2015, **54**, 1.
- 24 H. Virtanen, J. Yang, M. M. Bespalov, J. O. Hiltunen, V.-M. Leppänen, N. Kalkkinen, A. Goldman, M. Saarna and P. Runeberg-Ross, *Biochem. J.*, 2005, **387**, 817.